

# Numerical Evaluation of Multidirectional Wear in the UHMWPE tibial tray of Total Knee Prostheses

J. Bayod, M. A. Martínez and M. Doblaré

Group of Structural Mechanics and Material Modelling, Aragon Institute of Engineering Research (I3A)  
University of Zaragoza (Spain)

---

*The main responsible of the long-term failure of total knee replacements is wear of the UHMWPE component. Wear is associated to high contact pressures and relative displacements between the bearing surfaces and the multidirectional character of the sliding has a great importance. The main objective of this work is to analyze the importance of multidirectionality in wear of these components. Wear evolution has been predicted taking into account, or not, the multidirectional character of the relative sliding. Experimental tests have been used to fit the parameters of the models. Three-dimensional finite element models of four type of knee prostheses were developed in order to evaluate contact areas, pressures and relative slidings. Validation of the contact areas and pressures was made using data from experimental tests and commercial brochures. The results obtained showed an underestimation of up to a 64% on the wear depth when the multidirectional model was not considered.*

**Keyword:** total knee arthroplasty, ultra high molecular weight polyethylene, contact areas and pressures, wear, multidirectional sliding

---

## 1. INTRODUCTION

Wear of the bearing component, usually manufactured in ultra high molecular weight polyethylene, remains being the principal cause of long-term failure of knee prostheses, limiting the longevity of them [2, 19]. Although these clinical devices present survival rates of about 90% for a period of fifteen years, their increasing implantation in younger patients makes necessary to study this phenomenon to increase their durability. Wear causes the emission of small polyethylene particles leading to inflammation processes in the articulation [26, 39, 9]. These reactions produce resorption of the bones close to these prosthetic implants, phenomenon known as osteolysis, leading to the long-term loosening of the prosthesis and its posterior failure [34, 10, 46].

Wear is a material damage mechanism usually coupled with other damage processes like fatigue [36]. Contact pressures and relative displacements between the bearing surfaces are the main factors in promoting wear [45, 25]. Several approaches have been used to analyze wear of the polyethylene component, either through studies of removed implants [2, 16, 15], by experimental tests in vivo [35, 28], or by computational strategies [11, 40].

One of the problems of computational techniques relies on obtaining reliable contact pressure distributions on the polyethylene component. Some authors make use of the elastic foundation theory, also known as “bed of springs”, in multi-body dynamic models [11, 12], or between rigid bodies with softened contact [14].

Alternatively, full contact finite element schemes between deformable solids can also be considered [3, 24, 33, 37, 36]. Several studies may be found in the literature where finite elements are used to simulate the whole gait cycle [14, 31, 13], applying loads and displacement histories coming from knee simulators [43] or using standardized time-histories [17].

Most computational predictions of wear use the classical Archard’s law [1], which considers wear depth to be proportional to the module of the relative sliding between contact surfaces without taking into account changes in the direction of motion. In Total Knee Arthroplasty (TKA), however, although there exists a clear principal direction of sliding that corresponds to the anterior-posterior direction, sliding is actually multidirectional. This induces changes on the wear rate and causes a bigger volume of removed material when compared to a purely uniaxial approach [6, 27, 7, 44].

Hence, the aim of this work is to analyze the importance of the multidirectional character of sliding on the wear evolution in four different knee prostheses. Two wear models, uni and multidirectional, have been studied. Parameters of these wear models have been fitted by means of experimental tests on a Pin-on-Cylinder (POC) and on a Simplified Knee Simulator (SKS). Values of contact pressures and relative displacements were obtained by means of the finite element method using an implicit approach. Validation of the different models was accomplished by comparing the computed contact areas with values found in commercial brochures and/or obtained in experimental tests. Numerical results are good

comparing with commercial brochures (4.08%) and experimental tests (5.1%) for high loads. Finally, these models were applied to predict wear evolution in four prostheses. The results showed variations up to 64% between the two models.

## 2. MATERIAL AND METHODS

### 2.1. Geometrical and FE Models

In this work four knee prostheses from ZIMMER Inc. have been considered, all models belong to the Natural-Knee II<sup>®</sup> Family: Natural Knee II Congruent (NKC), Natural Knee II UltraCongruent (NKUC), Natural-Knee II Posterior Stabilized System (NKPS) and Natural Knee II Rotating Platforms (NKR). It should be noted that the first three are fixed bearing while the fourth is mobile bearing. The congruent model provides smaller contact areas than the others while the rotating platforms one gives rise to the biggest ones.

The geometries of the femoral and tibial components of the four prostheses previously listed, were reconstructed using *CATIA*<sup>™</sup> V5R7 (IBM, USA), from drawings supplied by ZIMMER. Finite element models of the polyethylene insert for NKC, NKUC and NKPS were composed of 23563, 47209, 52288 elements and 27199, 53941, 59160 nodes respectively (Figure 1). Finally, the rotating platform prosthesis is composed of three different parts: femoral component, tibial plateau and polyethylene insert. The latter was meshed with 45981 elements and 20474 nodes (Figure 2.a). Only surface meshes for the femoral component of the four models were generated since this component was considered fully rigid. Its mesh was composed of 20193 elements and 20150 nodes (Figure 3) while the tibial plateau was meshed with 10201 rigid elements and 33269 nodes. (Figure 2.b).

### 2.2. Constitutive Behavior

Due to the big difference in Young modulus between the metallic CrCo alloy and the polyethylene components (193 GPa versus 940 MPa), the former was approximated as a rigid solid while the latter was modelled as

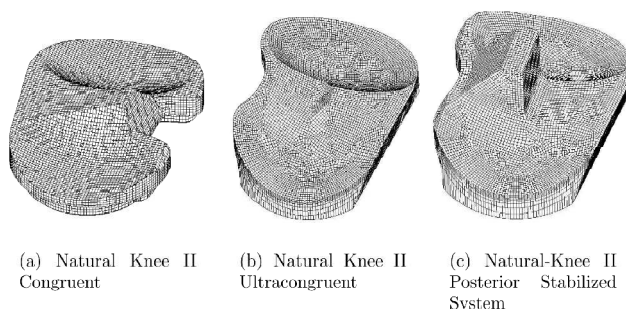


Figure 1: Finite Element Meshes of the polyethylene insert of the three fixed tray prostheses

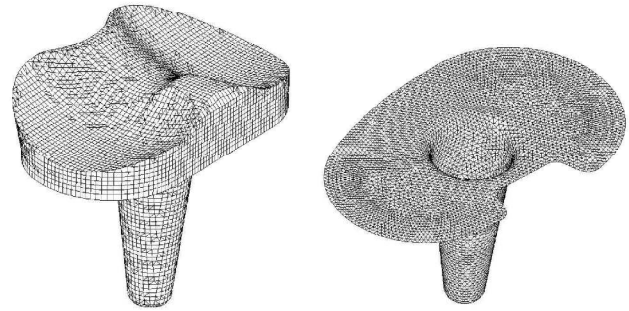


Figure 2: Prosthesis of Rotating Platforms

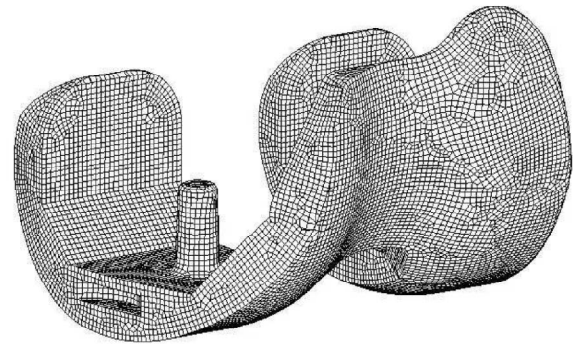


Figure 3: Femoral component for the four prostheses

deformable. This hypothesis is usual in the literature [29, 22]. Polyethylene was considered as a multi-linear elastic model with hardening defined by Kurtz [20], where ageing due to irradiation is considered. The stress-strain curve employed is included in Figure 4 and in Table 1.

Table 1  
Polyethylene constitutive parameters (see Fig. 4)

$E_i$	$T_i$
940.52 MPa	13.774225 MPa
401.255 MPa	21.74 MPa
157.5522 MPa	26.265 MPa
49.75	-

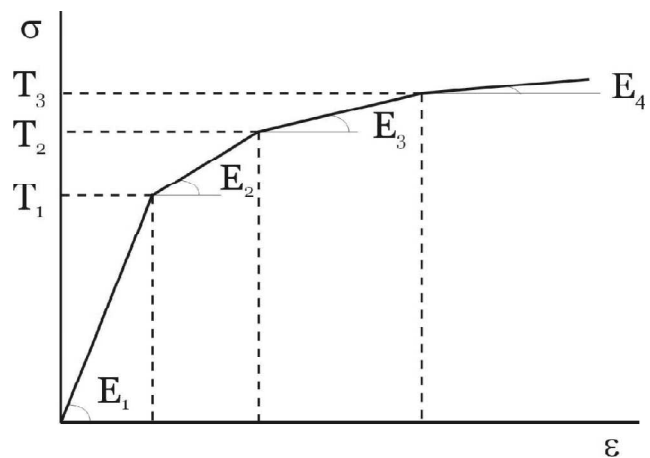


Figure 4: Polyethylene stress-strain curve

### 2.3. Loads and Boundary Conditions

Two different sets of loads were considered. The first consists of a compressive load in the femoral component acting at different fixed positions while the second is a load history corresponding to the whole gait cycle. The first set of analyses was employed to validate the finite element model comparing the obtained results with experimental ones or with data available in commercial brochures. The second load history was used to estimate the relative sliding history between the bearing components and posteriorly to predict polyethylene wear.

In the first set of analyses, the four prostheses were calculated at 0°, 15°, 60° and 90° flexion angles with imposed loads of 726 N, 2904 N, 3267 N and 3630 N along the vertical direction, corresponding to 4, 4.5 and 5 times the average body weight of a 60 years old, male patient [8, 32]. In order to validate the results obtained with the computational models described above, several experimental tests to determine the contact areas and pressures were developed for the NKUC, using the pressure-sensitive film technique (Fuji Film) [23]. The Fuji-film employed for these trials was Pressurex Film Low, with a sensitivity range from 2 to 10 N/mm<sup>2</sup> (285-1422 PSI). This film consists of two layers, the developer sheet and the ink-filled microcapsule sheet. This results

in red impressions on the developer sheet at points of contact. After the loading test, the marked films were removed and analyzed using a digital scanner and a computer software (Visilog) and obtain the contact areas after the corresponding calibration. As the condyles of this prosthesis are asymmetric, results for the medial and lateral condyles are obtained separately in addition to the global area value. The experimental tests are shown in Table 2.

**Table 2**  
**Experimental tests for the ultraconguent prosthesis**

Body Weight (BW)	Load (BW = 74 kg)	Flexion angle	Activity
4×BW	2904 N	0°, 15°	Gait cycle
5×BW	3630 N	60°	Stairs climbing
4.5×BW	3267 N	90°	Stairs descending

For the analyses reproducing the gait cycle, the imposed loads and flexion angles simulating the gait cycle were extracted from the ISO standard 14243-1 [17] (Figure 5). This cycle is composed of an axial load, an antero-posterior load cycle, a torque around the vertical direction and a flexion turn around the lateral-medial axis.

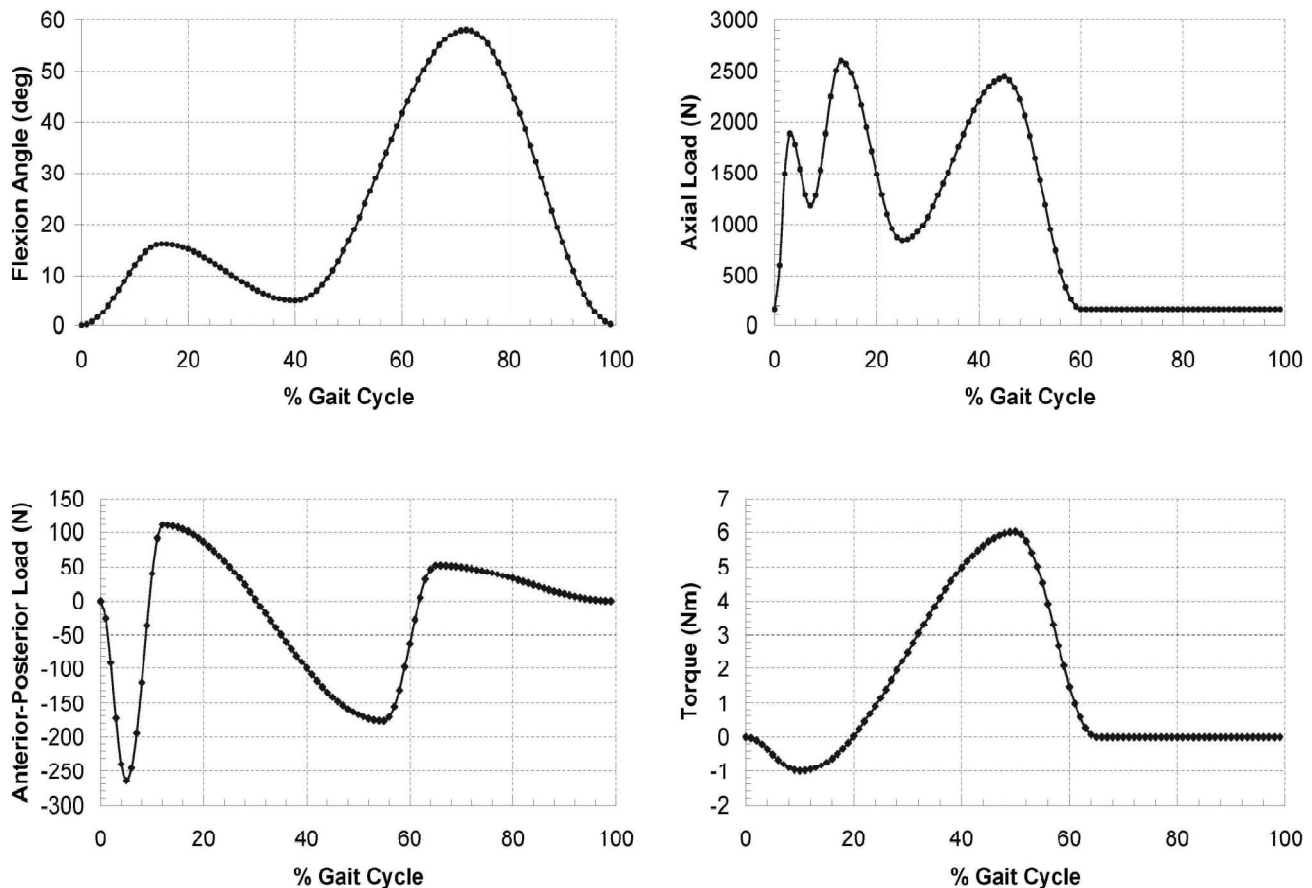


Figure 5: Loads and flexion angles during the gait cycle

## 2.4. Wear Models

The most used model to predict wear in mechanical components is the one proposed by Archard [?], that predicts the evolution of wear depth on a sliding contacting surface as:

$$\delta_{\text{wear}} = Nk \sum_{i=1}^n p_i d_i = k \sum p_i |v_i| \Delta t \quad (1)$$

where  $N$  is the number of the cycles,  $k$  is the wear rate of the material,  $p_i$  is the contact pressure and  $d_i$  is the amplitude of the relative sliding between contact surfaces computed by multiplying the instantaneous slip velocity  $v_i$  by the simulation time increment  $\Delta t$ .

Wang [44] and then Turrell *et al.* [41] slightly modified the Archard's approach to take into account the multidirectional character of sliding. In this work two wear models have studied. A more general model, initially proposed by Sawyer *et al.* [38], defines the wear rate  $k$  as a linear relationship with the parameter  $\sigma^*$ , that quantifies the intensity of the cross motion (2). A slight modification of this model is achieved by considering an exponential relation between  $k$  and  $\sigma^*$  (3).

$$k = k_n + k_m \sigma_i^* \quad (2)$$

$$k = e^{A+B \ln \sigma_i^*} \quad (3)$$

where  $k_n$ ,  $k_m$ ,  $A$  y  $B$  are experimentally determined fitting constants and  $\sigma^*$  is defined as the normalized crossing intensity:

$$\sigma_i^* = \sigma_i / \sigma_0 \quad (4)$$

being  $\sigma_i$  the crossing intensity, defined as

$$\sigma_i = \sqrt{\sum_{j=1}^n (\delta_j \Delta \theta_j)^2} / n \quad (5)$$

with  $\Delta \theta_j = \bar{\theta}_i - \theta_j$ .  $\bar{\theta}_i$  is the dominant orientation of tribological intensity defined as

$$\bar{\theta}_i = \frac{\sum_{j=1}^n \delta_j \theta_j}{\sum_{j=1}^n \delta_j} \quad (6)$$

where  $\theta_j$  indicates the instantaneous crossing orientation relative to a fixed medial-lateral axis.

Finally,  $\sigma_0$  is the worst-case crossing intensity defined for normalization purposes. The assumed worst-case situation is an uniform circular counterface motion. The wear depth of the material  $\delta_j$ , or tribological intensity, for each cycle  $i$ , is finally computed by the Archard's law:

$$\delta_i = k \sum_{j=1}^n p_j d_j = k \sum_{j=1}^n p_j |v_j| \Delta t \quad (7)$$

Two external programs were implemented into Visual C++ (*Visual C++*, *Version 6.0*) to evaluate the wear depth and wear volume as a post processing step. Needed data was extracted from Abaqus output files. The first script computes wear depth at each node, and the second one evaluates wear volume by using wear depth and a FE interpolation on the surface mesh. Updating of the mesh to include the remove of the wear material has not been considered in this analysis.

## 2.5. Experimental Tests to Fit the Wear Models

Two different experimental tests were developed to fit the constants of the wear models previously presented, a Pin-On-Cylinder (POC) test to fit the parameter of the Archard's law in a uniaxial sliding motion and different multidirectional tests developed on a Simplified Knee Simulator (SKS) that fit the multidirectional models.

The POC machine used in this experiment consists of a metallic disc and a UHMWPE cylindrical pin. A load of 150 N is applied while the disc turns (Figure 6.a). The SKS is an experimental machine based on the friction of a femoral head over a polyethylene flat plaque (Figure 6.b). The metallic head applies a vertical load of 500 N and suffers an oscillatory turn of  $\pm 45^\circ$ . Polyethylene keeps an "eight-form" oscillatory movement modelling an antero-posterior translation of  $\pm 5.5$  mm and an internal-external rotation of  $\pm 5^\circ$ . Every test consists of 5 millions of cycles.

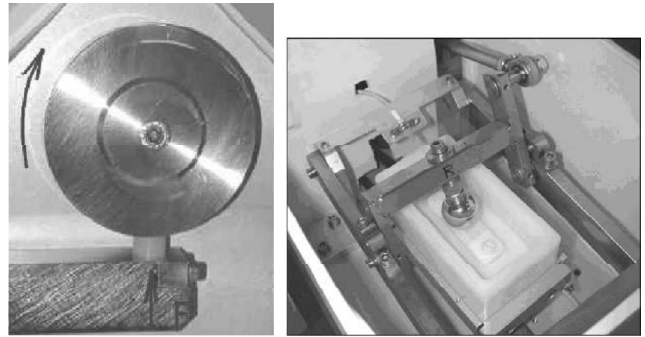


Figure 6: Pin-on-Cylinder and Simplified Knee Simulator

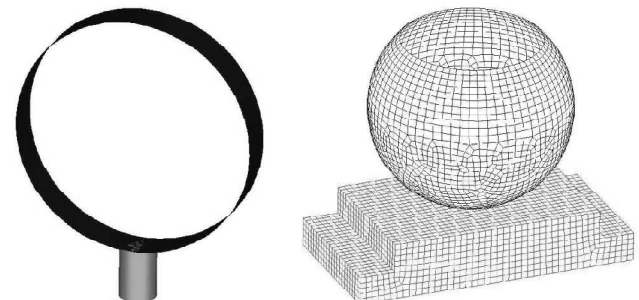


Figure 7: Finite element models for the Pin-on-Cylinder and the Simplified Knee Simulator tests

Finite element models for the POC and the SKS were developed to quantify the data needed to fit the wear models. For the POC, the disc and the polyethylene pin were modelled. Boundary conditions reproduced exactly the motions and restraints corresponding to the experimental test. The FE model of the SKS consists of two components: femoral head and polyethylene plate. Both models are shown in Figure 7. The disc and the femoral head were considered as a rigid solid.

### 3. RESULTS

#### 3.1. Validation of the Finite Element Models

The contact areas for the experimental tests and numerical analyses are shown in Table 3. The differences resulted lower than 15%, except for the case of 0° and 726 N. In such case, we believe that the experimental value was incorrect, since at 0° the prosthesis congruence is high. The pressure range of the film employed was from 2 to 10 MPa, so there is a non negligible zone with pressures lower than 2 MPa that the experimental technique is not able to capture, providing areas which are smaller than the actual ones, justifying the differences between experimental and numerical results.

The brochure of ZIMMER provides data for three positions (0°, 60 and 90° for 2904, 3630 and 3297 N, respectively). Our numerical results are very similar to those of the brochure, with an average error of 4.08%. The comparison amongst the results is shown in Figure 8.

**Table 3**  
Comparison between the experimental and numerical contact areas (mm<sup>2</sup>) obtained for the Ultracongruent prosthesis (NKUC)

	Flexion Angle			
	0°		15°	
	726 N	2904 N	726 N	2904 N
Medial Condyle	46	141.25	46.19	111.25
Lateral Condyle	55.61	180.06	46.87	116.49
Experimental	101.61	321.31	93.06	227.74
Numerical	192.5	354.6	108.4	214.8
Error %	47.21%	9.38%	14.15%	5.68%
	60°		90°	
	726 N	3630 N	726 N	3267 N
	726 N	3630 N	726 N	3267 N
Medial Condyle	42.78	122.51 N	35.32	83.21
Lateral Condyle	55.07	128.84	36.52	90.79
Experimental	97.85	251.35	71.84	174
Numerical	108.4	244.5	77.4	170.5
Error %	9.73%	2.72%	7.18%	2.87%

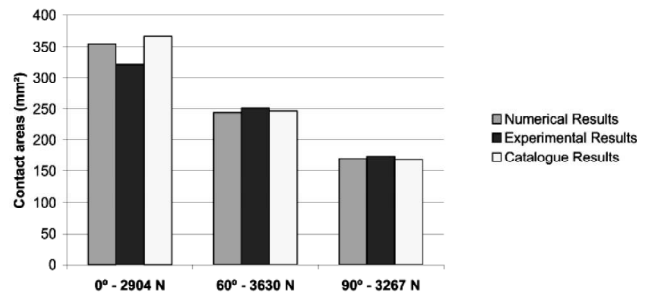


**Figure 8:** Comparison of contact areas [mm<sup>2</sup>] amongst numerical, experimental and brochure results for the ultracongruent prosthesis

#### 3.2. Contact Areas and Pressures Along the Gait Cycle

Contact areas and pressures are represented in Figures 9 and 10. NKUC and NKPS show very similar contact areas along the whole gait cycle, with average values of 135 and 138 mm<sup>2</sup>, and maximum values of 210 and 213 mm<sup>2</sup> respectively. NKRP always provides the highest contact areas with an average of 188 and a maximum of 404 mm<sup>2</sup>. Finally, NKC shows the lowest ones with an average value of 110 and maximum of 208 mm<sup>2</sup>. As expected, the lowest contact pressures appear in the NKRP for complete joint extension (Figure 10). On the other hand, NKC presents the lowest contact pressures, with a maximal pressure rather constant along the whole

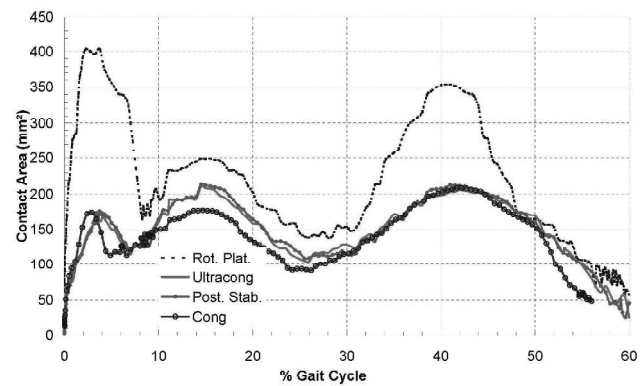


**Figure 9:** Contact areas for the four prostheses during the gait cycle [mm<sup>2</sup>]

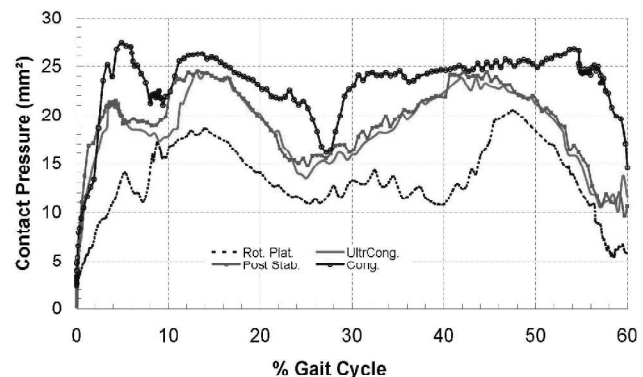


**Figure 10:** Maximal contact pressure for the four prostheses during the gait cycle [MPa]

cycle, close to 25 MPa. This results from the elastoplastic behaviour of the UHMWPE, presenting a behaviour curve practically flat at 26 MPa.

Figure 11 shows the anterior-posterior (A-P) displacement for each of the four prostheses studied. As in the results of areas and pressures, NKUC and NKPS show analogue performance with maximal values about -2 mm. NKC and NKRP show much higher A-P displacements. In the case of NKC, this is caused by the low congruence between the bearing surfaces. The contact zone is lower than in the other models, so the constraint the polyethylene finds to move with respect the femoral component is low. For NKRP, the polyethylene has no movement restriction but only those deriving from the contact of both metallic surfaces.

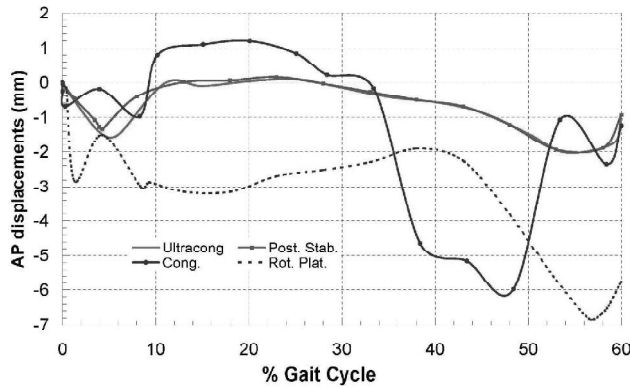


Figure 11: Anterior-Posterior displacement for the four prostheses [mm]

Internal-external rotations are shown in Figure 12. Again, NKUC and NKPS present similar values, with a maximum of 2 degrees. In the NKC higher angles appear, that may be explained again by the low congruence of the contact surfaces. For the NKRP, the tibial tray and the polyethylene component presented very different axial rotating angles. Polyethylene exhibited very low values while the tibial tray suffered important rotations. This is the consequence of the application of the anterior-posterior force and torque to the metallic tibial tray. These results were similar to other presented in the literature [30, 14, 13].

Table 4  
Values of constants for the three studied wear models

Archard's law	Linear Multi. Model	Exp. Multi. Model
$k = 2.814 \cdot 10^{-7}$	$k_n = 2.72 \cdot 10^{-7}$	$k_m = 1.05 \cdot 10^{-5}$
	$A = -19.55$	$B = 0.34$

### 3.3. Fitting of the Wear Models

The POC and SKS results data are employed to fit the constants of the wear models. So the estimation of the total volume wear is

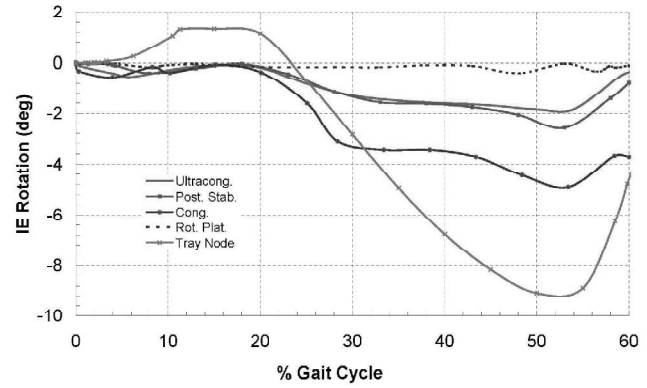


Figure 12: Axial rotation angle for the prostheses

$$\begin{cases} VolPOC = 6 \cdot 10^4 \int_A \sum_{i=1}^N (k_n + k_m \sigma_i^*) \delta_i dA \\ VolSim = 5 \cdot 10^6 \int_A \sum_{i=1}^N (k_n + k_m \sigma_i^*) \delta_i dA \end{cases} \quad (8)$$

$$\begin{cases} VolPOC = 6 \cdot 10^4 \int_A \sum_{i=1}^N \exp(A + B \ln \sigma_i^*) \delta_i dA \\ VolSim = 5 \cdot 10^6 \int_A \sum_{i=1}^N \exp(A + B \ln \sigma_i^*) \delta_i dA \end{cases} \quad (9)$$

where 60000 and 5 millions corresponds to the number of cycles for each test, and  $\delta_i$  is the wear depth for every cycle.

For the POC, 39 nine experimental tests were performed obtaining an average for polyethylene wear of  $0.040383 \text{ mm}^3/\text{km}$ . Using the FE approach, the better fitting of the  $k$  parameter of Archard's law results in  $2.814 \cdot 10^{-7} \text{ mm}^3/\text{Nm}$ . However, data from SKS are necessary for the multidirectional model. Average wear volume of the POC tests was  $86.46 \text{ mm}^3$  for 5 millions of cycles and the maximal contact pressure about 50 MPa. Values of the constants that better fit the two multidirectional models are presented in Table 4.

Figure 13 shows values of  $\sigma^*$  for the POC and SKS tests. Values of  $\sigma^*$  for the POC are nearly zero since it exhibits a clear unidirectional motion. On the other hand, SKS presents higher values of  $\sigma^*$  since its multidirectionality character is remarkable.

Table 5 shows the maximal wear depth and volume predicted by the numerical simulations. The Archard's law fits well the results of the POC tests but is not capable of evaluating correctly the SKS, being necessary to determine this volume with the model that takes into account the multidirectional character. The error found is 82%.

### 3.4. Wear Estimation

Numerical results of maximal wear depth and volume after one million cycles are shown in Table 6. Figures

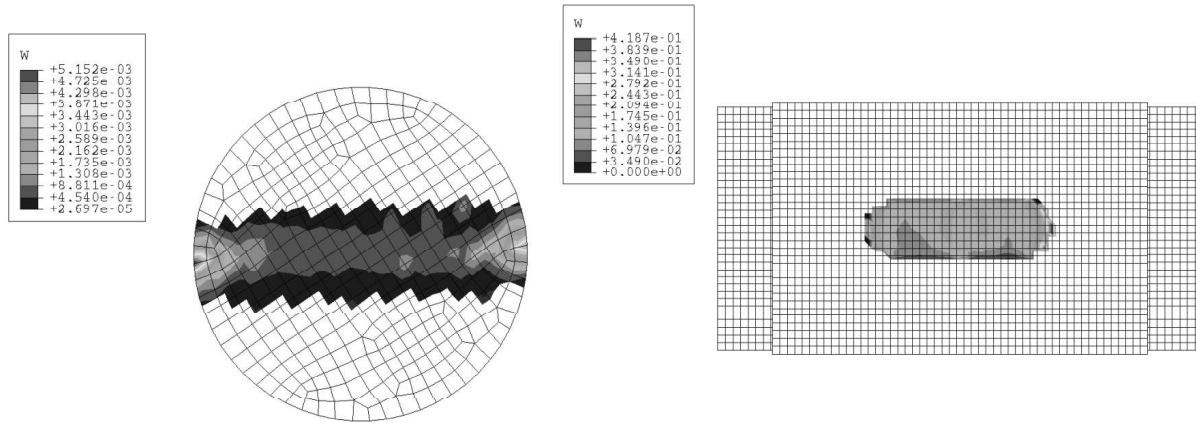


Figure 13:  $\sigma^*$  for POC and SKS experiments

**Table 5**  
Highest wear depth (mm) and weare volume (mm<sup>3</sup>) values for the POC and SKS tests

	Exp Results		Archard's law		Multidirectional Model		
	Volume	Depth	Volume	Depth	Linear Model	Exponential Model	
POC	0.44	0.047	0.449	0.055	0.449	0.055	0.450
SKS	86.69	0.401	15.38	2.63	86.69	2.38	86.57

16, 17 show the maximal wear depth contours for the Archard's law and linear multidirectional models, respectively. In all cases the congruent model presents the greatest wear depth, while the NKRP show the smallest ones. Comparing the wear volume, the four prosthesis present very similar volumes. However this effect is very different when comparing the results predicted by the multidirectional models. Now, the NKC presents the maximal wear volume, followed by the NKRP, NKPS and finally the NKUC.

Figure 14 shows the variable  $\bar{\theta}$  for the four prostheses. Logically, the predominant orientation is 90° for all the cases. However, it is observed that congruent and rotating platform prostheses present greater zones with values far from 90°, indicating a higher multidirectional motion. It is expected that these prostheses present higher wear estimation in the case of the multidirectional wear model.

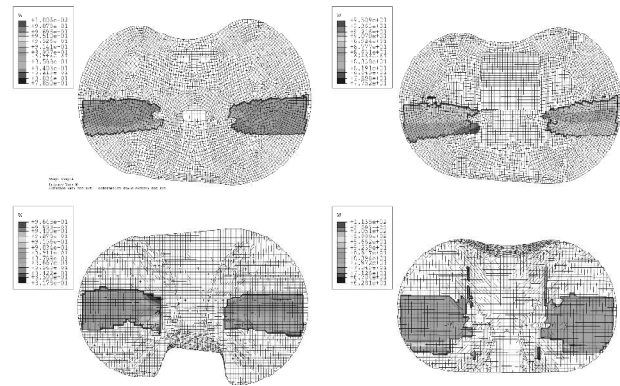


Figure 14:  $\bar{\theta}$  for the four prostheses

Contours for  $\sigma^*$  are shown in Figure 15. Values for NKUC are similar to NKPS with average values of 0.017 and 0.022. The NKC shows the highest average value of about 0.034. The NKRP presents average values of 0.028,

**Table 6**  
Maximal wear depth and wear volume results after one million cycles for the four prostheses

	Archard's law		Multidirectional model			
	Max. Depth	Volume	Linear Multi. Model		Exp. Multi. Model	
NKUC	0.085	11.15	0.171	19.72	0.284	33.82
NKPS	0.119	11.31	0.255	22.35	0.418	36.96
NKC	0.093	11.33	0.299	31.18	0.396	45.36
NKRP	0.071	11.31	0.135	24.68	0.229	39.30

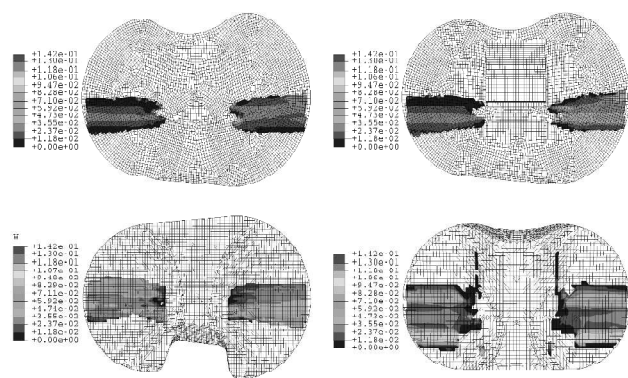


Figure 15:  $\sigma^*$  for the four prostheses

although it shows values very similar to NKUC and NKPS in most of the bearing surface, it presents higher values in the posterior zone where the tribological intensity is very small so it has a low influence in the final wear depth.

4. DISCUSSION AND CONCLUSIONS

The main objective of this work is to study the importance of multidirectional motions in wear of the polyethylene insert in TKA. Four models of prostheses have been studied, three with fixed and one with mobile bearing

platforms. A gait cycle was reproduced to obtain contact pressures and relative sliding between the contacting surfaces. Fundamental variables like contact areas and pressure and relative sliding of the bearing surfaces have been analyzed. The evaluation of wear has been carried out following two different models, taking into account or not, the multidirectional character of the sliding. Experimental tests on a POC and on a SKS machines have been made to fit the parameters of the two wear models.

Contact areas resulted higher for the NKRP during the whole cycle. NKUC and NKPS presented a similar performance and the NKC showed the smallest contact areas. With respect to contact pressures, NKRP showed the lowest values in the whole cycle and NKC the highest. These results agree with those found by different authors [30, 14, 42, 13] although the prostheses evaluated by these authors were not the same studied in this work. So, the results obtained are not completely comparable. Contact pressures also agreed with that found by Otto *et al.* [31], who obtained a pressure of 17 MPa at 13% of the gait cycle for a rotating platform prosthesis. NKUC and NKPS gave rise to similar values (24 MPa at 13% of the gait cycle) and between those of the NKRP (17.5 MPa) and NKC (26 MPa). Kinematics of NKUC and NKPS was again very similar. NKC and NKRP showed higher relative sliding and axial rotation angles.

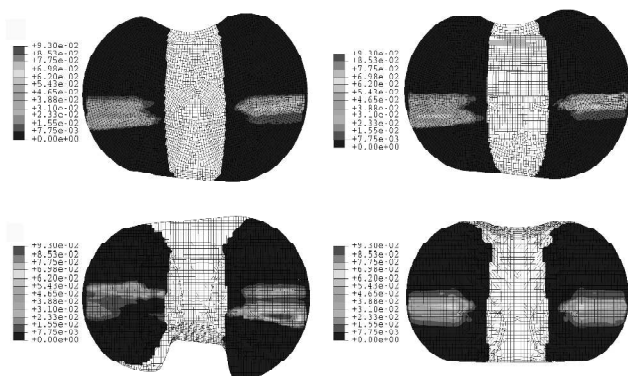


Figure 16: Wear depth after one million cycles for the four models using the Archard's law

Table 7  
Difference in % of the removed material volume ( $mm^3$ ) between Archard's law and linear multidirectional model

Prosthesis	Unidir.	Linear	Difference (%)	Exp. multidir
NKUC	11.15	19.72	43.46	33.82
NKPS	11.31	22.35	49.40	36.96
NKC	11.33	31.18	63.66	45.36
NKRP	11.31	24.68	54.17	37.30

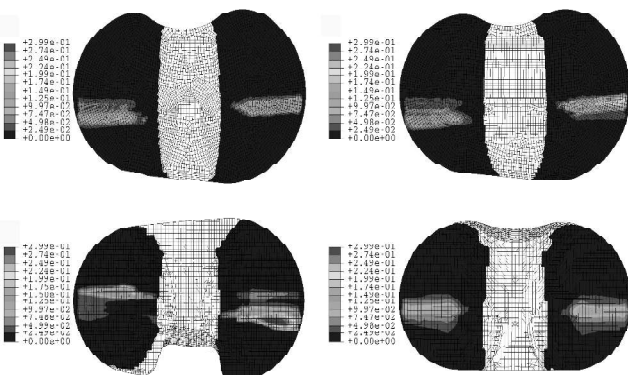


Figure 17: Wear depth after one million cycles for the four models using the linear multidirectional model

Regarding the estimation of wear of UHMPWPE, the Archard's law predicts values very similar for the four models analyzed, about 11  $mm^3$  after one million cycles, appearing remarkable differences amongst them when the multidirectional character is considered and higher respect to the Archard's model. NKUC presents the smallest value, NKC the biggest and NKPS and NKRP similar and intermediate between the other two. These results are similar to other found in the literature [2, 18, 21]. Table 7 shows these differences, that can be as high as 64%. The highest difference appears for the NKC prosthesis due to the high multidirectional motion of this low congruence model.

NKRP exhibits a wear volume close to NKUC and NKPS but slightly higher. Although NKRP presents a higher degree of congruence than the fixed bearing models, the relative slidings are more marked. Analogous results are found by some authors [18, 21], presenting similar wear for fixed and mobile bearing prosthesis. Possibly, higher differences amongst these two models could be found in other activities like stairs climbing or descending, where the congruence is very different at high flexion angles. Therefore, consideration or not of the multidirectional character of sliding can drive to remarkable differences in the estimation of wear.

We have found that the exponential model estimates a wear volume bigger than those found in the literature. On the contrary, the multidirectional linear model gives more appropriate results comparing with other experimental results previously published. Nevertheless, these experimental results were obtained from different prosthesis models and materials, so further experimental tests with this geometries and materials are needed to better fit parameters of the wear model and to validate some of the results we present in this investigation.

It is important to remark some limitations of this study. A simplified kinematics of the articulation, taken from standards, has been considered. A more complete analysis considering the actual kinematics of the joint would be needed to obtain a more specific study. For example, considering data coming from inverse dynamics analysis obtained from volunteers using a motion capture system and load platform. In order to fully simulate the global performance of the joint it will be necessary to introduce the complete geometry of the knee components: bones, ligaments, tendons, etc, with reliable material behaviours. Moreover, the loads and boundary conditions could be obtained from in-vivo kinematics, i.e. motion capture devices and inverse dynamics or fluoroscopy. Instead of only a gait cycle, other activities, such as stairs climbing or descending could be also considered. The characterization of the wear models have been performed employing only two types of experimental tests, POC and SKS. It would be desirable to carry out further experiments for a better characterization. Another possible limitation is the simplified modelling of the UHMWPE behaviour. Some more complex constitutive models have been reported, including  $J_2$  plasticity, viscoplastic phenomena or dependence on cyclic loading [4, 5]. However the differences amongst the models are not expected to be too high in this range of stresses (0-20 MPa). Some authors have also studied the influence of removing the wearied material by modifying the finite element mesh [47].

#### ACKNOWLEDGMENTS

The authors gratefully acknowledge the research support of the Spanish Ministry of Science and Technology through the research

project DPI2006-14669 and Zimmer Inc. for providing the drawings of the different prostheses.

#### REFERENCES

- [1] J. F. Archard and W. Hirst. The wear of metals under unlubricated conditions. *Proceedings of the Royal Society of London*, A236: 397-410, 1956.
- [2] T. Ashraf, J. H. Newman, V. V. Desai, D. Beard, and J. E. Nevelos. Polyethylene wear in a non-congruous unicompartmental knee replacement: a retrieval analysis. *The Knee*, 11: 177-181, 2004.
- [3] D. L. Bartel, J. J. Rawlinson, A. H. Burstein, C. S. Ranawat, and W. F. Flynn. Stresses in polyethylene components of contemporary total knee replacements. *Clinical Orthopaedics and Related Research*, 317: 76-82, 1995.
- [4] J. S. Bergstrom, C. M. Rimnac, and S. M. Kurtz. Prediction of multiaxial mechanical behavior for conventional and highly crosslinked UHMWPE using a hybrid constitutive model. *Biomaterials*, 24: 1365-1380, 2003.
- [5] J. S. Bergstrom, C. M. Rimnac, and S. M. Kurtz. An augmented hybrid constitutive model for simulation of unloading and cyclic loading behavior of conventional and highly crosslinked UHMWPE. *Biomaterials*, 25: 2171-2178, 2004.
- [6] C. R. Bragdon, D. O. O'Conner, J. D. Lowenstein, M. Jasty, and W. D. Syniuta. The Importance of Multidirectional Motion on the Wear of Polyethylene. *Journal of Engineering in Medicine*, 210: 157-165, 1996.
- [7] B. R. Burroughs and T. A. Blanchet. Factors Affecting the Wear of Irradiated UHMWPE. *Tribol. Trans.*, 44: 215-223, 2001.
- [8] K. Diem and C. Lentner. *Scientific Tables*. Ciba Geigy Limited, Switzerland, 1973.
- [9] J. H. Dumbleton, M. T. Manley, and A. A. Edidin. A literature review of the association between wear rate and osteolysis in total hip arthroplasty. *The Journal of Arthroplasty*, 17: 649-661, 2002.
- [10] J. Fisher, H. M. J. McEwen, P. I. Barnett, C. Bell, M. H. Stone, and E. Ingham. Influences of sterilising techniques on polyethylene wear. *The Knee*, 11: 173-176, 2004.
- [11] B. Fregly, Y. Bei, and M. Sylvester. Experimental evaluation of an elastic foundation model to predict contact pressures in knee replacements. *Journal of Biomechanics*, 36: 1659-1668, 2003.
- [12] B. J. Fregly, W. G. Sawyer, M. K. Harman, and S. A. Banks. ComputationalWear Prediction of a Total Knee Replacement from In Vivo Kinematics. *Journal of Biomechanics*, 2004.
- [13] A. C. Godest, M. Beaugonin, E. Haug, M. Taylor, and P. J. Gregson. Simulation of a knee joint replacement during a gait cycle using explicit finite element analysis. *Journal of Biomechanics*, 35: 267-275, 2002.
- [14] J. P. Halloran, A. J. Petrella, and P. J. Rullkoetter. Explicit finite element modeling of total knee replacement mechanics. *Journal of Biomechanics*, 38: 323-331, 2005.
- [15] M. K. Harman, S. A. Banks, and W. A. Hodge. Polyethylene damage and knee kinematics after total knee arthroplasty. *Clinical Orthopaedics and Related Research*, 392: 383-393, 2001.
- [16] A. Hoshino, Y. Fukuoka, and A. Ishida. Accurate in vivo measurement of polyethylene wear in total knee arthroplasty. *The Journal of the Arthroplasty*, 17: 490-496, 2002.
- [17] ISO. *ISO/FDIS 14243-1*. Final Draft International Standard, 2001.

- [18] T. S. Johnson, M. P. Laurent, J. Q. Yao, and C. R. Blanchard. Comparison of wear of mobile and fixed bearing knees tested in a knee simulator. *Wear*, 255: 1107-1112, 2003.
- [19] D. J. Kilgus. Polyethylene Wear in Mobile-Bearing Prostheses. *Orthopedics*, 25: 227-233, 2002.
- [20] S. M. Kurtz, D. L. Bartel, and C. Rimnac. Postirradiation aging affects stress and strain in polyethylene components. *Clinical Orthopaedics*, 350: 209-220, 1998.
- [21] C. J. Lavernia, R. J. Sierra, D. S. Hungerford, and K. Krackow. Activity Level and Wear in Total Knee Arthroplasty. *The Journal of Arthroplasty*, 16: 446-453, 2004.
- [22] J. J. Liao, C. K. Cheng, C. H. Huang, and W. H. Lo. The effect of malalignment on stresses in polyethylene component of total knee prostheses—a finite element analysis. *Clinical Biomechanics*, 17: 140-146, 2002.
- [23] A. B. Liggins, W. R. Hardie, and J. B. Finlay. The spatial and pressure resolution of fuji pressure-sensitive film. *Experimental Mechanics*, 35: 166-173, 1995.
- [24] D. D. D' Lima, P. C. Chen, and Jr. C. W. Colwell. Polyethylene Contact Stresses, Articular Congruity, and Knee Alignment. *Clinical Orthopaedics and Related Research*, 392: 232-238, 2001.
- [25] G. Liu, Y. Chen, and H. Li. A study on sliding wear mechanism of ultrahigh molecular weight polyethylene/next tempolypropylene blends. *Wear*, 256: 1088-1094, 2004.
- [26] J. M. Mirra, R. A. Mardes, and Amstutz. The pathology of failed total joint arthroplasty. *Clin Orthop*, 170: 175-183, 1982.
- [27] O. K. Muratoglu, C. R. Bragdon, D. O. O'Connor, M. Jasty, W. H. Harris, R. Gul, and F. McGarry. Unified Wear Model for Highly Crosslinked Ultra-High Molecular Weight Polyethylene. *Biomaterials*, 20: 1643-1470, 1999.
- [28] O. K. Muratoglu, R. S. Perinchief, C. R. Bragdon, D. O. O'Connor, R. Konrad, and W. H. Harris. Metrology to Quantify Wear and Creep of polyethylene Tibial Knee Inserts. *Clinical Orthopaedics and Related Research*, 410: 155-164, 2003.
- [29] J. Otto, J. Callaghan, and T. Brown. Contact mechanics influences on interface mobility of a rotating platform total knee. *Bioengineering Conference*, 50: 779-780, 2001.
- [30] J. K. Otto, J. J. Callaghan, and T. D. Brown. Mobility and Contact Mechanics of a Rotating Platform Total Knee Replacement. *Clinical Orthopaedics and Related Research*, 392: 24-37, 2001.
- [31] J. K. Otto, J. J. Callaghan, and T. D. Brown. Gait Cycle Finite Element Comparison of Rotating-Platform Total Knee Designs. *Clinical Orthopaedics and Related Research*, 410: 181-188, 2003.
- [32] P. D. Postak, C. S. Heim, and A. S. Greenwald. Tibial Plateau Surface Stress in TKA: A Factor Influencing Polymer Failure Series II. *62nd Annual AAOS Meeting*, 1, 1995.
- [33] J. J. Rawlinson and D. L. Bartel. Flat medial-lateral conformity in total knee replacements does not minimize contact stresses. *Journal of Biomechanics*, 35: 27-34, 2002.
- [34] P. A. Revell, B. Weightman, M. A. Freeman, and B. V. Roberts. The production and biology of polyethylene wear debris. *Arch Orthop Trauma Surg*, 91: 167-181, 1978.
- [35] V. Saikko and O. Calonius. Simulation of wear rates and mechanisms in total knee prostheses by ball-on-flat contact in a five-station, three-axis test rig. *Wear*, 253: 424-429, 2002.
- [36] S. Sathasivam and P. S. Walker. Computer Model to Predict Subsurface Damage in Tibial Inserts of Total Knees. *Journal of Orthopaedic Research*, 16: 564-571, 1998.
- [37] S. Sathasivam and P. S. Walker. The conflicting requirements of laxity and conformity in total knee replacement. *Journal of Biomechanics*, 32: 239-247, 1999.
- [38] W. G. Sawyer, M. A. Hamilton, M. C. Sucec, B. J. Fregly, and S.A. Banks. Quantifying multidirectional sliding motions in total knee replacements. *Transactions of the ASME*, 127: 280-286, 2005.
- [39] T. P. Schmalzried, M. Jasty, and W. H. Harris. Periprosthetic bone loss in total hip arthroplasty: polyethylene wear debris and the concept of the effective joint space. *J Bone Joint Surg*, 74A: 849-863, 1992.
- [40] S. H. Teoh, W. H. Chan, and R. Thampuran. An elasto-plastic finite element model for polyethylene wear in total hip arthroplasty. *Journal of Biomechanics*, 35: 323-330, 2002.
- [41] M. Turrell, A. Wang, and A. Bellare. Quantification of the effect of cross-path motion on the wear rate of ultra-high molecular weight polyethylene. *Wear*, 255: 1304-1039, 2003.
- [42] T. Villa, F. Migliavacca, D. Gastaldi, M. Colombo, and R. Pietrabissa. Contact stresses and fatigue life in a knee prosthesis: comparison between in vitro measurements and computational simulations. *Journal of Biomechanics*, 37: 45-53, 2004.
- [43] P. Walker, G. Blunn, D. Broome, J. Perry, A. Watkins, S. Sathasivam, M. Dewar, and J. Paul. A knee simulating machine for performance evaluation of total knee replacements, *Journal of Biomechanics*, 30: 89-89, 1997.
- [44] A. Wang. A Unified Theory of Wear for Ultra-High Molecular Weight Polyethylene in Multi-Directional Sliding. *Wear*, 248: 38-47, 2001.
- [45] M. A. Wimmer and T. P. Andriacchi. Tractive forces during rolling motion of the knee: implications for wear in total knee replacement. *Journal of Biomechanics*, 30: 131-137, 1997.
- [46] T. M. Wright and S. B. Goodman. *Implant Wear in Total Joint Replacement*. American Academy of Orthopaedic Surgeons, 2001.
- [47] J. Shih-Shyn Wu, J. P. Hung, C. S. Shu, and J. H. Chen. The computer simulation of wear behavior appearing in total hip prosthesis. *Computer Method and Programs in Biomedicine*, 70: 81-91, 2003.